Setup for investigating gold nanoparticle penetration through reconstructed skin and comparison to published human skin data

Hagar I. Labouta
Sibylle Thude
Marc Schneider

Setup for investigating gold nanoparticle penetration through reconstructed skin and comparison to published human skin data

Hagar I. Labouta,[a,c] **Sibylle Thude,**[d] **and Marc Schneider**[b]
[a]Helmholtz Center for Infection Research, Helmholtz Institute for Pharmaceutical Research Saarland, Saarbrücken, Germany
[b]Saarland University, Department of Pharmaceutical Nanotechnology, Saarbrücken, Germany
[c]University of Alexandria, Department of Pharmaceutics, Alexandria, Egypt
[d]Fraunhofer Institute for Interfacial Engineering and Biotechnology (IGB), Stuttgart, Germany

Abstract. Owing to the limited source of human skin (HS) and the ethical restrictions of using animals in experiments, *in vitro* skin equivalents are a possible alternative for conducting particle penetration experiments. The conditions for conducting penetration experiments with model particles, 15-nm gold nanoparticles (AuNP), through nonsealed skin equivalents are described for the first time. These conditions include experimental setup, sterility conditions, effective applied dose determination, skin sectioning, and skin integrity check. Penetration at different exposure times (two and 24 h) and after tissue fixation (fixed versus unfixed skin) are examined to establish a benchmark in comparison to HS in an attempt to get similar results to HS experiments presented earlier. Multiphoton microscopy is used to detect gold luminescence in skin sections. $\lambda_{ex} = 800$ nm is used for excitation of AuNP and skin samples, allowing us to determine a relative index for particle penetration. Despite the observed overpredictability of penetration into skin equivalents, they could serve as a first fast screen for testing the behavior of nanoparticles and extrapolate their penetration behavior into HS. Further investigations are required to test a wide range of particles of different physicochemical properties to validate the skin equivalent-human skin particle penetration relationship. © *2012 Society of Photo-Optical Instrumentation Engineers (SPIE).* [DOI: 10.1117/1.JBO.18.6.061218]

Keywords: particle penetration; skin equivalent; colloidal gold; multiphoton microscopy, skin penetration.

Paper 12567SS received Aug. 30, 2012; revised manuscript received Nov. 7, 2012; accepted for publication Nov. 7, 2012; published online Nov. 30, 2012.

1 Introduction

Investigation of skin penetration of nanoparticles is a hot research topic. This is of significance in health risk analysis, in addition to designing optimal topical and transdermal nano-carriers and biomedical diagnostic agents.[1,2] Yet most of the attention was given to defining the status of skin nanoparticle penetration and implementing new approaches to enhance their penetration, rather than setting up a universal standard test for more reliable results. This has created a state of dilemma with many conflicting results, as highlighted in several reviews by DeLouise,[1] Labouta and Schneider,[2] and Schneider et al.[3]

Human skin (HS) is regarded as the gold standard and the most reliable skin model for *in vitro* penetration studies,[4] either for active molecules[5] or for nanoparticles.[6–8] However, due to the limited source of HS for many research laboratories, animal skin was used as an alternative skin model for conducting these experiments. Comparing the different skin models from different origins to human skin regarding drug penetration revealed that monkey and pig skins are better models than the skin of rodents.[9] For ethical reasons, primate research is restricted, and pig skin is preferred, as it can be readily obtained as waste from animals slaughtered for food.[9] Therefore, pig skin was extensively used as a surrogate for HS for testing nanoparticle penetration, especially when follicular penetration is in scope.[10–12] Artificially reconstructed human skin or "skin equivalents" (SE) represent another alternative skin model for conducting penetration/permeation experiments.

The past years have witnessed an increase in the number of commercially available SE, such as EpiSkin® (previously manufactured by Episkin, Chaponost, France, and now by L'Oreal, SkinEthic, Nice, France), SkinEthic® (L'Oreal, SkinEthic, Nice, France), EpiDerm® (MatTek, Ashland, Massachusetts), AST-2000 (CellSystems, St. Katharinen, Germany), and Apligraf® (Organogenesis Inc., Canton, Massachusetts).[13] These models are generally comprised of HS cells grown as tissue culture and matrix equivalents normally present in skin. They were found to be good models for testing skin irritation, phototoxicity, and skin metabolism.[13,14] For drug transport testing, however, many studies have revealed that the permeability of reconstructed skin models is much higher compared with excised human skin, because of less well-developed barriers.[15] Nevertheless, the reconstructed skin models available today are useful tools for estimating the rank order of percutaneous absorption of a series of compounds with different physicochemical properties.[16] Moreover, these skin models clearly appear superior with respect to the reproducibility of data.[17] This would offer a more robust setup than human or animal skin tissues, which suffer strongly from inter-individual and intra-individual (according to site) variations.

To the best of our knowledge, there is only one study so far investigating the penetration of 7-nm quantum dots through SE

Address all correspondence to: Marc Schneider, Saarland University, Department of Pharmaceutical Nanotechnology, Campus A4 1, D-66123 Saarbrücken, Germany. Tel: +49 681 302 2438; Fax: +49 681 302 4677; E-mail: Marc.Schneider@mx.uni-saarland.de

followed by tape stripping and visualization of the tape strips by means of fluorescence microscopy. Though these models are generally known to overestimate drug flux across skin relative to HS, no penetration of nanoparticles was reported in this particular study.[18] Yet the results obtained were not justified in this context and were not compared to HS experiments conducted in the same research laboratory.

Multiphoton microscopy is one of the most important recent inventions in biological imaging, enabling noninvasive three-dimensional study of biological specimens. Multiphoton excitation is a nonlinear process in which a fluorophore is excited by two or more photons simultaneously at a wavelength in the near-infrared region.[19–22] Multiphoton imaging of noble metal nanoparticles, e.g., gold nanoparticles (AuNP), has emerged as a potential alternative to the fluorophore-labeled particles. This technique is referred to as multiphoton-absorption-induced luminescence (MAIL), where the absorption of multiple photons from a near-infrared pulsed femtosecond laser can lead to robust luminescence of metal nanoparticles.[8,23–26] Multiphoton microscopy was therefore employed as a useful optical technique to track particle penetration in skin[8,22,26–28] and was the imaging tool in our study to track model AuNP.

The aim of this study was therefore designing a test to examine the potential skin penetration of nanoparticles under standardized reproducible conditions using a three-dimensional tissue-cultured skin model. For these models, primary human keratinocytes were exchanged with immortalized human keratinocyte cell line, HaCaT, to improve the reproducibility and consistency of the developed skin models, reducing intra-batch and inter-batch variations. This data would then allow comparison of results obtained using SE with previous experiments on full-thickness HS we conducted with the same particles in our laboratory,[7,8] thus eliminating inter-laboratory variations. AuNP were chosen as a good model for studying skin penetration of nanoparticles due to their unique optical properties[23,26,29,30] in addition to their potential as drug carriers.[31,32]

2 Materials and Methods

2.1 Preparation and Characterization of Gold Nanoparticles

Ionically stabilized, polar AuNP were prepared according to the Turkevich method.[33] In short, a 70-ml solution of hydrogen tetrachloroaurate (HAuCl$_4 \cdot$ 3H$_2$O, Sigma-Aldrich Chemie GmbH, Steinheim, Germany) containing about 100 μg/ml gold was brought to boiling under magnetic stirring and then reduced by a solution of trisodium citrate dihydrate (Na$_3$C$_6$H$_5$O$_7 \cdot$ 2H$_2$O, Sigma-Aldrich) containing five-fold the molar concentration of the gold salt. After the gold colloid formation, its temperature was lowered to room temperature. The colloid was then transferred into a suitable glass container and stored in the refrigerator protected from light.

The optical properties of the prepared AuNP were checked using a UV/Vis Spectrophotometer (lambda 35, Perkin Elmer, Rodgau-Jürgesheim, Germany) in the range of 400 to 800 nm. The particles were also characterized, as indicated in our previously published work,[7] in terms of mean particle size and morphology by TEM (JEOL Model JEM 2010, JEOL GmbH, Eching, Germany) and the zeta potential based on the electrophoretic mobility (Zetasizer Nano, Malvern Instruments, Malvern, United Kingdom).

2.2 Constructing a Skin Equivalent From Human Foreskin Fibroblasts and HaCaT Cells (Keratinocytes)

A reconstructed SE was grown from human foreskin fibroblasts and HaCaT keratinocytes according to the following protocol: Collagen gel (extracted from rat tail in 0.1% acetic acid) containing human fibroblasts was pipetted on the top of a cell culture insert [Greiner BioOne, Frickenhausen, Germany (pore size: 1.0 μm, PET membrane)] in a six-well cell culture plate. The fibroblast-containing gel was cultured for one day at 37°C and 5% CO$_2$ under submersed conditions, applying a total of 2.5 ml Dulbecco's Modified Eagle's medium (Life Technologies GmbH, Darmstadt, Germany) with 10% fetal calf serum (FCS) (Life Technologies GmbH, Darmstadt, Germany) per well and insert.

The following day, a volume of 50 μL fibronectin (Life Technologies GmbH, Darmstadt, Germany) solution (5 μg/ml) was then added and incubated again for 10 min at 37°C. HaCaT keratinocytes (CLS Cell Lines Service, Eppelheim, Germany; tested for mycoplasma) in 100 μL keratinocyte growth medium-2 (KGM-2 Kit) (Promocell, Heidelberg, Germany) with 5% FCS were subsequently seeded on top of the collagen gels. After 1 h of incubation at 37°C, a total of 2.5 ml KGM-2 medium containing FCS (5%) was added to each insert. While maintaining submersed culture conditions, medium was exchanged on day 3, 4, and 5, thereby gradually lowering the FCS concentration from 5% to 0%. At the end of the submersed culture period (day 7), inserts with the skin equivalents were transferred into six-well cell culture plates. KGM-2 medium without human epidermal growth factor and bovine pituitary extract but supplemented with calcium chloride solution (Sigma-Aldrich, Taufkirchen, Germany), 1.88 mM, was filled into each well up to the level of the insert membrane (air-lift culture). The air-lift culture was performed for up to 13 days, with medium exchange performed every second day. One skin construct was then used for histological examination to check the formation of the skin layers.

The skin construct should then be used within four to five days, during which the culture medium should be changed daily.

2.3 Skin Penetration Study of AuNP Through Skin Equivalents

2.3.1 Penetration of AuNP through nonfixed skin equivalents

The culture medium was carefully removed, and specimens were washed with freshly prepared phosphate buffer saline, pH 7.4, three times. Specimens on their PET inserts (polyethylene terephthalate membrane, pore size diameter: 1 μm) were then transferred into a new six-well plate, where skin penetration study was conducted. The receptor (basolateral)/surrounding compartment was filled with 800 μL KRB, touching the tissue from below (Fig. 1). AuNP, with a concentration of 90 μg/ml, was carefully applied on the top of the skin surface, in the center to avoid leakage to the deeper skin layers (DSL). The plate was then covered with parafilm and plastic cover and maintained at 37°C, 5% CO$_2$ throughout the experiment (2 or 24 h). Following exposure, the skin surface was gently cleaned with a tissue. Collected skin was examined after longitudinal cryo-sectioning. All experiments were done in triplicates.

Defining the system:
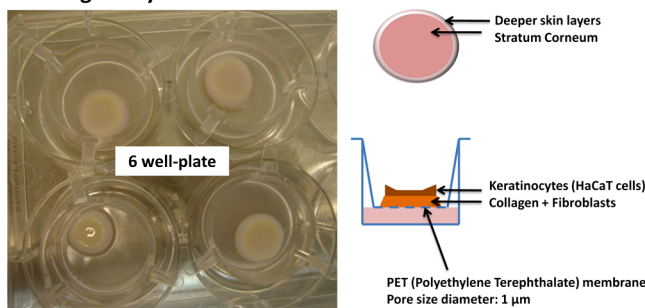
Fig. 1 Setup and skin model used for testing nanoparticle penetration. The skin model was developed *in vitro* from HaCaT cells on the top of fibroblasts in collagen. This developed into an open-edged nonsealed specimen with concave surface.

2.3.2 *Penetration of AuNP through fixed skin equivalents*

The culture medium was carefully removed, and specimens were washed three times, followed by incubation in 4% formalin in phosphate buffer saline for 30 min. Specimens were then treated similarly.

2.3.3 *Skin integrity test*

For each penetration experiment, one specimen was used to check the effect of the test conditions on the specimen integrity. This was done by treating the specimens similar to test specimens. This, however, was followed by applying methylene blue on the top of the specimen for 1 h and checking for permeation to the basolateral compartment versus a control insert without skin specimen.

2.4 *Longitudinal Skin Cryo-Sectioning*

Skin cross-sections were performed at −26°C using a cryo-microtome (Slee, Mainz, Germany). Following fast freezing of the skin specimen, an 8-mm punch in the center of the specimen was placed in a perpendicular direction to the cutting blade to avoid dislocation of the particles from outside into the tissue or vice versa, thus limiting sectioning artifacts.[28] Skin sections were placed on microscopy slides and mounted by an aqueous mounting medium (FluorSaveTM reagent, Calbiochem, San Diego) and covered with glass cover slips.

2.5 *Multiphoton Microscopy*

Imaging was performed using an inverted confocal/two-photon excitation fluorescence microscope (ZEISS LSM 510 META NLO system, Carl Zeiss, Jena, Germany) equipped with a tunable pulsed NIR laser to evoke nonlinear optical excitation processes (Chameleon, Coherent, Dieburg, Germany). The objective used was a water immersion lens 63X (NA = 1.2) with a working distance of around 200 μm. A wavelength of 800 nm was used for both excitation of AuNP and scanning the skin samples using 0.485 and 0.647 mW, respectively. The energy was measured in the focal plane of the microscope after the objective using a power meter. The pulse width at the laser output was less than 140 fs, and the repetition frequency was 80 MHz (specified by Coherent). The gain settings were adjusted for each measurement individually. The optical settings, discussed in detail earlier,[26,28] allowed for a clear separation of both signals from AuNP and the tissue with no signal

interference among tracks, as shown earlier.[28] Z-stacks of the skin samples were taken with steps every 1 μm. Each optical scan is composed of 512×512 pixels and a size of 0.14×0.14 μm^2. The gain settings were adjusted for each measurement individually.

2.6 *Data Analysis*

The method of semiquantitation of nanoparticles in skin is based on measuring the frequency or the number of pixels due to the detected gold luminescence signal in the *Stratum Corneum* (SC) and DSL. A detailed description of the method of analysis for the acquired *z*-stacks has been published earlier,[28] and so has a detailed protocol.[34] Briefly, the number of pixels of AuNP signals as semiquantitative data for the distribution of AuNP in the SC and viable DSL were determined ($\sum$Pixel) for each optical layer (1-μm thickness) of a respective *z*-stack of the examined longitudinal skin sections. The overall sum from all optical sections was calculated and biased by the theoretical optical size and the pixel size to obtain the number of AuNP in the different skin layers to compare different experiments according to Eq. (1):

$$N_w = \frac{\sum \text{Pixel} \times A_{\text{pixel}}}{A_{\text{particle}}}, \qquad (1)$$

where A_{pixel} (area of one pixel) $= 0.139 \times 0.139$ μm^2, and A_{particle} (area of diffraction-limited image spot due to AuNP) $= \sim 0.365$ μm^2, based on the optical settings used in this study, as detailed elsewhere.[28]

It should be noted here that the summed value developed by data analysis is regarded as a semiquantitative index to compare penetration into the SC and DSL under the same conditions, as well as for different formulations and conditions. Summed values were found more informative than mean values (SD) due to the nonhomogeneous distribution of the particles throughout the diffusion area. This has been explained in detail earlier.[7] This value does not give the real amount of particles penetrated.

2.7 *Setting up the Experimental Conditions*

Nanoparticle penetration experimentation through skin equivalent was standardized in terms of the experimental setup, sterility level, applied dose/area, cryo-sectioning conditions, and skin integrity check. This will be discussed in detail in the following section.

3 Results and Discussion

To overcome a shortage of HS, a protocol for testing drug permeation was previously developed and validated according to the organisation for economic co-operation and development (OECD) principles[35] using three commercially available types of reconstructed human epidermis. Permeability was compared to that of human epidermis, pig skin, and bovine udder skin using nine compounds with different physicochemical characteristics. Their results showed that these reconstructed epidermal SE can be used for drug permeation studies, taking into account product-specific overpredictability.[36,37] However, a protocol for testing nanoparticle penetration through SE has not been issued yet. Figure 1 shows the setup and a skin model we developed and used for testing nanoparticle penetration. It should be noted here that, even though the seeded cell dispersions (collagen
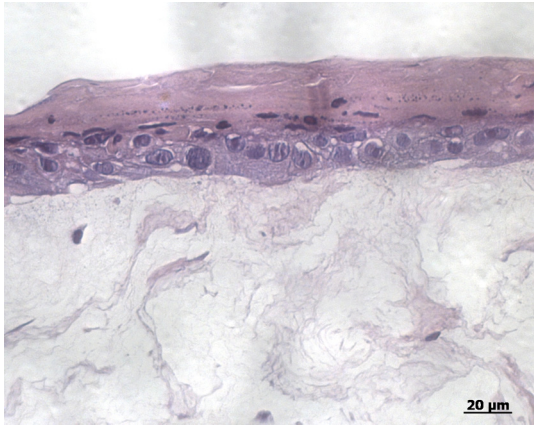
Fig. 2 Hematoxylin and eosin stained section of the developed full-thickness skin equivalent.

sponge seeded with fibroblasts and HaCaT cells) initially covered the whole area, they grew to nonsealed open-edged skin constructs. This is typical for collagen-based full-thickness skin substitutes, due to low mechanic resilience.[38] Figure 2 shows a histological cross-section of the developed SE stained by hematoxylin and eosin.

AuNP [hydrophilic, negatively charged (zeta potential -35.1 ± 1.9 mV), citrate-stabilized, $\varnothing = 14.9 \pm 1.8$ nm] were fully characterized as indicated in our previously published work.[7] They were selected for this study because they were shown not to penetrate HS after 24 h of skin contact and were exclusively localized in the SC.[7,8] This would facilitate comparison of results of both skin models. In addition, mere treatment of tissue-cultured skin favors application of hydrophilic particle dispersions, rather than exposure to hydrophobic particles dispersed in organic solvent.

Prepared and characterized AuNP were then applied to the developed SE at a concentration of 90 μg/ml for a skin exposure time of 2 and 24 h. After the skin penetration experiment, skin punches were longitudinally sectioned and analyzed using multiphoton microscopy.

The main principle behind imaging of gold nanoparticles was discussed in several previous studies.[23–25] Based on this, we developed a method to detect AuNP in skin.[8,26,28] Though multiphoton microscopy is a nondestructive optical technique, skin sectioning was required to avoid the possible limitations when imaging from the top view in case of nonsectioned skin specimens in which AuNP could be detected up to variable depths from the skin surface ranging from 14 to 100 μm, depending on skin pre-treatment (tissue fixation) and area of examination (presence or absence of wrinkles).[26] Representative optical z-stacks were then analyzed as mentioned in the methodology to determine the weighted number of particles in the SC and DSL.[28] It should be noted here that the proposed methodology does not guarantee single-particle detection based on the resolution of the microscope under the imaging conditions; 0.5 ± 0.1 and 1.0 ± 0.3 μm in the lateral and axial resolutions, respectively, as measured in our previous study.[26] The effect of aggregation on the measurements was discussed in that study. Low probability of aggregation was assumed based on similar results obtained on imaging different particle concentrations, knowing that aggregation is a phenomenon that is dependent on concentration. Moreover, the relative

obtained values are of significance, rather than the absolute figures.

The main focus of this work was to standardize all the experimental conditions for conducting a successful particle penetration experiment using the developed SE model. The following are the main points considered while developing the test conditions, as shown in Fig. 3(a).

3.1 Experimental Setup

The Franz diffusion cell, the most common setup for conducting a penetration/permeation experiment, was not used in this case to avoid shear stress on the skin specimen developing from clamping the receptor and donor compartments together. On the contrary, experiments were run in a six-well plate with inserts in which the basolateral compartment was equivalent to the receptor compartment in the Franz diffusion cell, and particle dispersion was applied on the top of the specimen. Open-edged nonsealed specimens in the insert did not result in leakage of the applied red AuNP colloid, due to the concave surface of the SC that holds the applied dispersion (Fig. 1).

It should be noted here that using Franz diffusion cells in skin permeation studies through reconstructed human epidermis is possible, as has already been shown previously.[36] Special inserts could be used to avoid the shear stress on the epidermis. However, this is not possible for full-thickness *in vitro* tissue, due to thickness variations from one specimen to another. In addition, the low mechanical resistance of this skin model is due to the usage of collagen, which is not the case for other skin models (no dermis), and thus Franz diffusion cells cannot be used in this case.

3.2 Sterility Conditions

Already formed skin tissue should be still kept under strictly sterile conditions before and during the penetration experiment; otherwise, infection may occur, leading to loss of barrier properties, as shown in Fig. 3(a-ii), in which infection has led to loss of specimen's ability to retain the applied AuNP and their complete leakage outside the specimen.

3.3 Measurement of the Diffusion Area

Contraction of the skin constructs on growth was not uniform for all skin specimens, resulting in different diffusion areas, as shown in Fig. 3(a-iv). Therefore, the dose was standardized per diffusion area. Prior to the penetration experiment, the skin specimen was imaged, and the diffusion area was estimated from the area of a circle of the same area with the help of the freeware program Image J (http://rsbweb.nih.gov/ij/) reference to a standard scale bar.

3.4 Skin Sectioning

Shear stress should be minimized as much as possible while sectioning to avoid artifacts. Many trials were conducted to have good skin cuts. For this, the whole skin punch was completely embedded and surrounded by binding solution, Tissue-Tek® (Sakura Finetek Europe, Zoeterwoude, Netherlands), on the specimen block on cryo-sectioning. This minimizes stress on edges. Moreover, skin punch should be sectioned at a minimum thickness of 50 μm. Thinner sections were not possible without detaching SC and DSL, as shown in Fig. 3(a-v). This does not reflect on the poor quality of the used skin models, since 10-μm
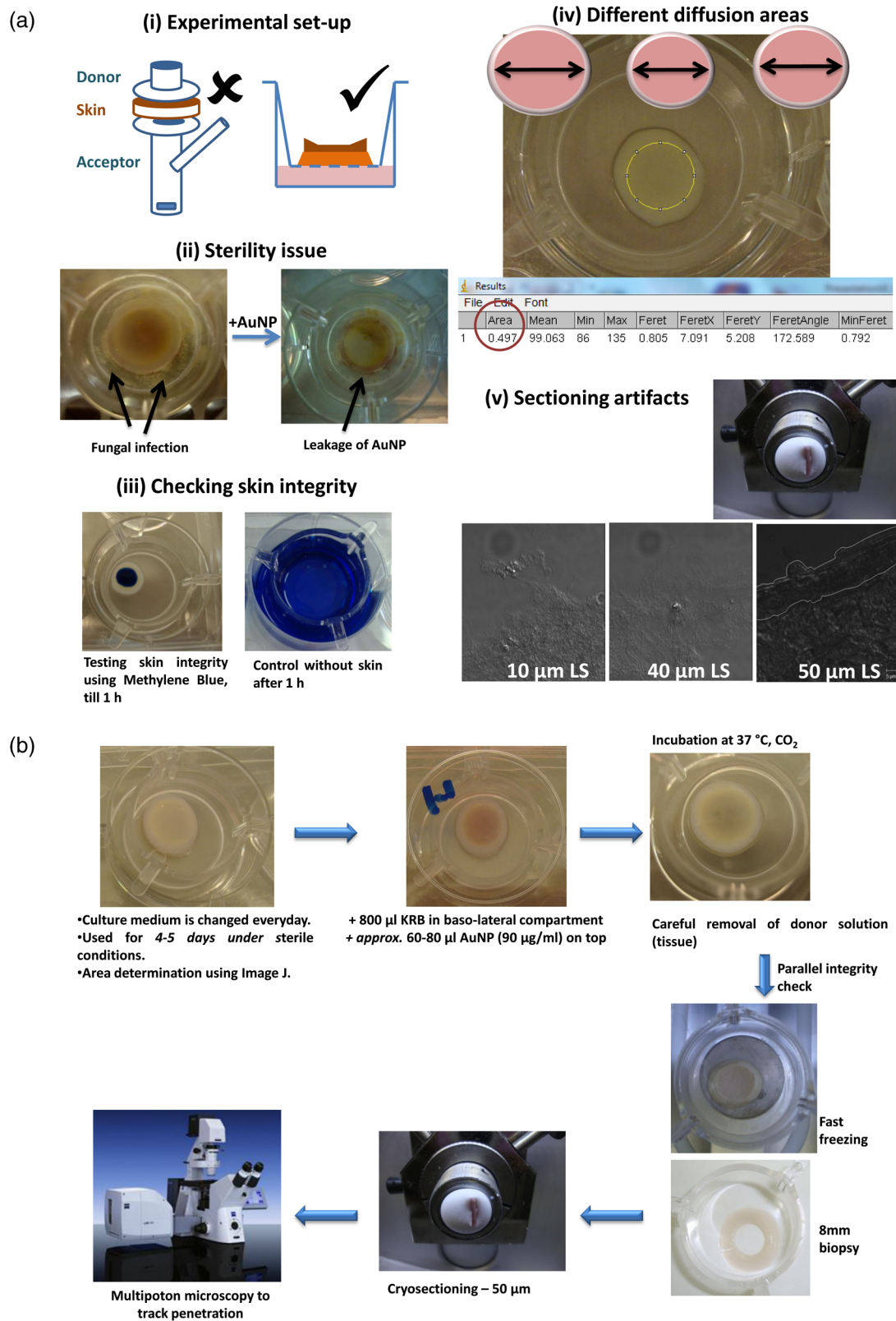
Fig. 3 (a) Criteria for conducting a particle penetration experiment through the reconstructed skin. (i) The Franz diffusion cell was found not to be a suitable model for the reconstructed skin to avoid excess pressure on the tissue leading to detached *Stratum Corneum* and loss of the skin barrier function. (ii) Working under unsterile conditions could result in fungal or bacterial infection, loss of the barrier function of the SC, and thus leakage of the applied particles to the surrounding area. (iii) For each batch of reconstructed skin tissues, one skin piece was used for testing skin integrity by means of methylene blue. (iv) The applied dose was standardized for the surface area of the SC determined prior to conducting the penetration experiment. (v) On skin cryo-sectioning prior to microscopical examination, the skin piece should be entirely surrounded by embedding solution to eliminate stress on skin edges, and the skin is cut at a thickness of 50 μm. Thinner skin sections could result in skin artifacts (loss of integrity). (b) An optimal experimental setup is thus proposed.
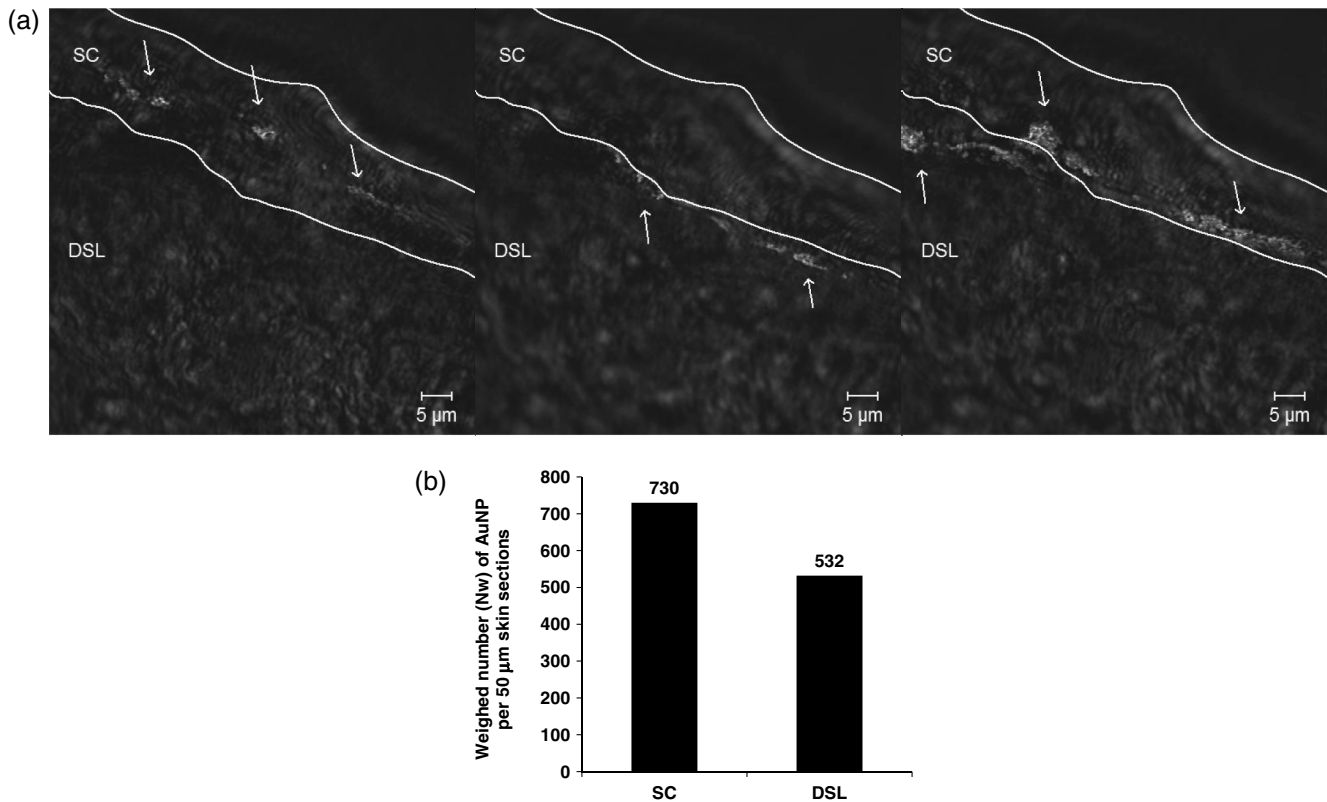
Fig. 4 (a) Representative overlaid multiphoton/transmission images showing gold nanoparticles (indicated as white spots) at different optical layers of a z-stack of a longitudinal skin section, in which different amounts of gold nanoparticles in the *Stratum Corneum* and deeper skin layers after 24 h of skin exposure were detected in each layer. A single layer was therefore not descriptive for the overall penetration pattern, due to nonhomogeneous distribution. (b) The weighted number of particles in all optical layers of the z-stack was thus determined, as shown above, showing the depth profile for AuNP concentrating more in the SC rather than in DSL.

sections of control untreated skin samples of the same model were possible to cut, as has been shown previously.[26] This is also not due to a deleterious effect of gold nanoparticles on the skin model, since skin samples grown in presence of gold nanoparticles could be cut in >10-μm sections.[26] However, this could be due to the increased swelling of the skin tissue after long incubation time with gold nanoparticle dispersion.

The skin integrity check was performed as mentioned in the methodology. For all the test conditions, the barrier function of the SE was not distorted, as shown in Fig. 3(a-iii).

Figure 3(b) shows the optimal procedure followed when performing a particle penetration experiment through nonsealed SE. Table 1 compares these conditions with that of HS experiments performed in our laboratory. The penetration experiment was then conducted under these optimal experimental conditions for 24 h exposure time. Similar to HS experiments,[7] results showed nonhomogeneous distribution of AuNP all over the diffusion area, as shown in Fig. 4(a). Therefore, analysis was not dependent on one image field, as explained previously by the method of image analysis we developed earlier.[28] However, analysis of z-stacks showed depth profiles of AuNP having higher values in the upper skin layer and SC, and decreasing toward the DSL, as shown in Fig. 4(b). On comparing the number of particles penetrating into the SC and DSL in HS and SE experiments (Table 1), one could conclude an overpredictability of the SE model. This underlines again the structural deficit of reconstructed skin regarding the barrier quality (density). A seven-fold increase in the number of particles in the SC of SE versus HS was observed. In SE experiments, the particles

were not exclusively localized in the SC but penetrated further into the DSL. This is despite the fact that the effective dose of particles topically applied was lower for the SE experiment than in the comparable HS experiment (Table 1). Overprediction was also the case observed for previously reported drug permeation experiments through commercial SE.[13,36,37] This implies a similar behavior of molecules and particles when penetrating the skin, but a lower penetration rate is expected here, due to the particulate nature and the reduced diffusion.[3] This presumption is supported by our previously published work.[6,7]

Attempts were therefore adopted to counteract the overpredictability of SE experiments for particle penetration. Two variables were tested: exposure time and tissue fixation.

Exposure of SE to AuNP for a shorter time (2 h versus 24 h) resulted in exclusive localization of AuNP in the SC with no penetration into the DSL (Fig. 5). This result is equivalent to the 24 h penetration experiment through HS (Table 1). This could be positively employed as a fast test in the future for testing the penetration of topically applied nanoparticles, especially for cosmetic preparations, and extraplate this to penetration through HS. However, further experiments are required to validate the relationship, especially for other nanoparticles with different materials and surface chemistries.

Tissues constructed *in vitro* (SE, in this case) could possibly suffer low compactness; i.e., compact organization is not easy to attain for artificially constructed skin. However, the use of fixatives was previously shown to be effective in the structural preservation of SE.[39] Therefore, the effect of fixation on increasing the tissue density was examined as a method to limit particle

Table 1 Comparison between skin penetration experiments through human skin and skin equivalent in terms of experimental conditions and penetration results.

	HS experiment	SE experiment
Setup	Franz diffusion cell	Six-well plate experiment
Temperature	32°C	37°C, CO_2
Donor solution	500 μl (constant)	60 to 80 μl (variable)
Diffusion area	1.76 cm^2 (constant)	Approx. 0.73 cm^2 (variable)
Applied volume/ area	284.1 $\mu L/cm^2$ (constant) About 4 times SE exp.	Approx. 75.34 $\mu L/cm^2$ (variable)
Receptor solution	12 ml PBS, pH 7.4	800 μL KRB, pH 7.4
Longitudinal sections	10 μm	50 μm
Penetration of AuNP	No penetration (24 h)	Penetration (24 h) No penetration (2 h)
Semiquantitation (24 h) [Particles/ 10 μm skin section]	SC: 21 particles DSL: None	SC: 146 particles DSL: 106
Penetration depth (24 h)	SC	VE
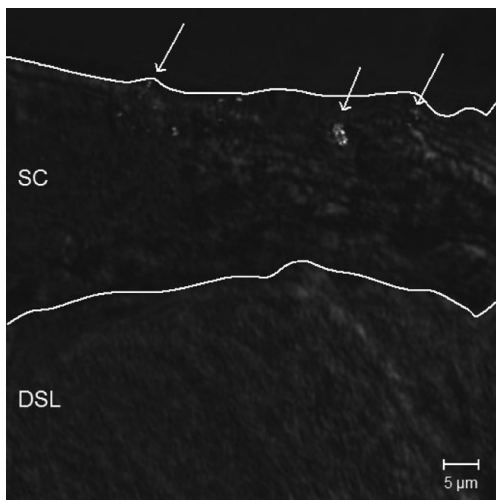
Fig. 5 Representative overlaid multiphoton/transmission image showing exclusive localization of gold nanoparticles (indicated as white spots) in the *Stratum Corneum* after 2 h of skin exposure and no penetration into the deeper skin layers.

penetration. On the contrary, skin fixation resulted into a two-fold increase in particle localization in the SC and a slight increase in the frequency of particles penetrating into the DSL relative to unfixed skin tissues exposed to AuNP for the same exposure time, 24 h (Fig. 6). A greater enhancement effect was even evident on shorter exposure time, 2 h, in which tissue fixation resulted in induction of penetration into the DSL, versus exclusive localization for unfixed specimens, as well as a 56-fold increase in the number of particles in the SC (Fig. 6).
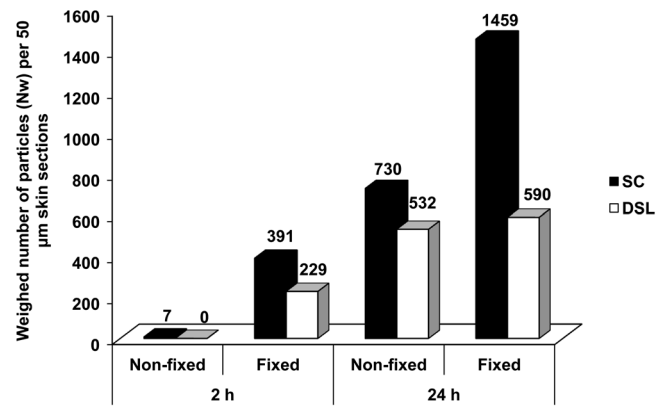
Fig. 6 The effect of skin fixation on the penetration of gold nanoparticles after time exposures of two and 24 h, as extracted from optical layers of z-stacks (1 μm step width) imaged by multiphoton microscopy.

This could be explained by the higher effect of formalin as a severe skin irritant, resulting in diminished barrier function rather than being a skin fixative. Nevertheless, skin fixation was found not to be a suitable method to avoid the exaggerated particle penetration results through SE.

4 Conclusion

Standardized experimental conditions for conducting particle penetration experiments through nonsealed SE were developed for the first time. Critical factors tested affecting penetration included skin exposure time and tissue fixation. In short penetration experiments, 2 h could be enough to predict penetration through HS. In the future, a range of different particles of different physicochemical parameters should be examined concomitant to equivalent HS penetration experiments at different exposure times to study the different penetration behavior of the particles. The main expected challenge is the limited range of dispersion media that could be applied on tissue-engineered skin without diminishing skin integrity, e.g., hydrophobic particles dispersed in organic solvents. It should be also mentioned here that the developed skin model does not take into account follicular penetration. Furthermore, it was shown that excised human skin gives different results regarding hair follicle penetration compared to *in vivo* investigations, due to shrinkage of the hair follicles *in vitro* on cutting.[40]

References

1. L. A. Delouise, "Applications of nanotechnology in dermatology," *J. Invest. Dermatol.* **132**(3 Pt. 2), 964–975 (2012).
2. H. I. Labouta and M. Schneider, "Interaction of inorganic nanoparticles with the skin barrier: current status and critical review," *Nanomed. Nanotechnol. Biol. Med.* (2012) (in press).
3. M. Schneider et al., "Nanoparticles and their interactions with the dermal barrier," *Dermatoendocrinol.* **1**(4), 197–206 (2009).
4. B. Godin and E. Touitou, "Transdermal skin delivery: Predictions for humans from *in vivo*, *ex vivo* and animal models," *Adv. Drug Deliv. Rev.* **59**(11), 1152–1161 (2007).
5. H. I. Labouta and L. K. El-Khordagui, "Polymethacrylate microparticles gel for topical drug delivery," *Pharm. Res.* **27**(10), 2106–2118 (2010).
6. H. I. Labouta, L. K. El-Khordagui, and M. Schneider, "Could chemical enhancement of gold nanoparticle penetration be extrapolated from established approaches for drug permeation?," *Skin Pharmacol. Phys.* **25**(4), 208–218 (2012).
7. H. I. Labouta et al., "Mechanism and determinants of nanoparticle penetration through human skin," *Nanoscale* **3**(12), 4989–4999 (2011).

8. H. I. Labouta et al., "Gold nanoparticle penetration and reduced metabolism in human skin by toluene," *Pharm. Res.* **28**(11), 2931–2944 (2011).

9. A. M. Barbero and H. F. Frasch, "Pig and guinea pig skin as surrogates for human *in vitro* penetration studies: a quantitative review," *Toxicol. Vitro* **23**(1), 1–13 (2009).

10. M. Ossadnik et al., "Investigation of differences in follicular penetration of particle-and nonparticle-containing emulsions by laser scanning microscopy," *Laser Phys.* **16**(5), 747–750 (2006).

11. A. Patzelt et al., "Selective follicular targeting by modification of the particle sizes," *J. Control. Release* **150**(1), 45–48 (2011).

12. A. Vogt et al., "40 nm, but not 750 or 1,500 nm, nanoparticles enter epidermal CD1*a*+ cells after transcutaneous application on human skin," *J. Invest. Dermatol.* **126**(6), 1316–1322 (2006).

13. S. Pappinen et al., "Organotypic cell cultures and two-photon imaging: tools for *in vitro* and *in vivo* assessment of percutaneous drug delivery and skin toxicity," *J. Control. Release* **161**(2), 656–667 (2012).

14. F. Netzlaff et al., "The human epidermis models EpiSkin®, SkinEthic® and EpiDerm®: an evaluation of morphology and their suitability for testing phototoxicity, irritancy, corrosivity, and substance transport," *Eur. J. Pharm. Biopharm.* **60**(2), 167–178 (2005).

15. S. P. Huong et al., "Use of various models for *in vitro* percutaneous absorption studies of ultraviolet filters," *Skin Res. Technol.* **15**(3), 253–261 (2009).

16. M. Van Gele et al., "Three-dimensional skin models as tools for transdermal drug delivery: challenges and limitations," *Exp. Opin. Drug Deliv.* **8**(6), 705–720 (2011).

17. A. Gysler, U. Königsmann, and M. Schäfer-Korting, "Tridimensional skin models recording percutaneous absorption," *ALTEX* **16**(2), 67–72 (1999).

18. S. H. Jeong et al., "Assessment of penetration of quantum dots through *in vitro* and *in vivo* human skin using the human skin equivalent model and the tape stripping method," *Biochem. Bioph. Res. Commun.* **394**(3), 612–615 (2010).

19. F. Helmchen and W. Denk, "Deep tissue two-photon microscopy," *Nat. Methods* **2**(12), 932–940 (2005).

20. P. T. So et al., "Two-photon excitation fluorescence microscopy," *Annu. Rev. Biomed. Eng.* **2**, 399–429 (2000).

21. A. Diaspro, G. Chirico, and M. Collini, "Two-photon fluorescence excitation and related techniques in biological microscopy," *Quart. Rev. Biophys.* **38**(02), 97–166 (2005).

22. F. Stracke et al., "Multiphoton microscopy for the investigation of dermal penetration of nanoparticle-borne drugs," *J. Invest. Dermatol.* **126**(10), 2224–2233 (2006).

23. R. A. Farrer et al., "Highly efficient multiphoton-absorption-induced luminescence from gold nanoparticles," *Nano. Lett.* **5**(6), 1139–1142 (2005).

24. D. Nagesha et al., "*In vitro* imaging of embryonic stem cells using multiphoton luminescence of gold nanoparticles," *Int. J. Nanomedicine* **2**(4), 813–819 (2007).

25. M. B. Dowling et al., "Multiphoton-absorption-induced-luminescence (MAIL) imaging of tumor-targeted gold nanoparticles," *Bioconjug. Chem.* **21**(11), 1968–1977 (2010).

26. H. I. Labouta et al., "Depth profiling of gold nanoparticles and characterization of point spread functions in reconstructed and human skin using multiphoton microscopy," *J. Biophotonics* **5**(1), 85–96 (2012).

27. T. R. Kuo et al., "Chemical enhancer induced changes in the mechanisms of transdermal delivery of zinc oxide nanoparticles," *Biomaterials* **30**(16), 3002–3008 (2009).

28. H. I. Labouta et al., "Combined multiphoton imaging-pixel analysis for semiquantitation of skin penetration of gold nanoparticles," *Int. J. Pharm.* **413**(1–2), 279–282 (2011).

29. V. Kirejev et al., "Multiphoton microscopy—a powerful tool in skin research and topical drug delivery science," *J. Drug Deliv. Sci. Technol.* **22**(3), 250–259 (2012).

30. N. Reum et al., "Multilayer coating of gold nanoparticles with drug-polymer coadsorbates," *Langmuir* **26**(22), 16901–16908 (2010).

31. L. Dykman and N. Khlebtsov, "Gold nanoparticles in biomedical applications: recent advances and perspectives," *Chem. Soc. Rev.* **41**(6), 2256–2282 (2012).

32. H. I. Labouta and M. Schneider, "Tailor-made biofunctionalized nanoparticles using layer-by-layer technology," *Int. J. Pharm.* **395**(1–2), 236–242 (2010).

33. J. Turkevich, P. C. Stevenson, and J. Hillier, "A study of the nucleation and growth processes in the synthesis of colloidal gold," *Discuss Faraday Soc.* **11**, 55–75 (1951).

34. H. I. Labouta, U. F. Schaefer, and M. Schneider, "Laser scanning microscopy approach for semiquantitation of *in vitro* dermal particle penetration," in *Molecular Dermatology: Methods and Protocols*, C. Has and C. Sitaru, Eds., p. 594, Humana Press, New York (2013).

35. OECD, "Draft Guideline 428: Skin absorption: *in vitro* method," in *OECD Guideline for the Testing of Chemicals* (2004).

36. M. Schäfer-Korting et al., "The use of reconstructed human epidermis for skin absorption testing: Results of the validation study," *Altern. Lab Anim.* **36**(2), 161–187 (2008).

37. M. Schäfer-Korting et al., "Reconstructed human epidermis for skin absorption testing: results of the German prevalidation study," *Altern. Lab Anim.* **34**(3), 283–294 (2006).

38. F. Groeber et al., "Skin tissue engineering—*in vivo* and *in vitro* applications," *Adv. Drug Deliv. Rev.* **63**(4–5), 352–366 (2011).

39. H. R. Choi et al., "The fixation of living skin equivalents," *Appl. Immunohistochem. Mol. Morphol.* **14**(1), 122–125 (2006).

40. J. Lademann et al., "Which skin model is the most appropriate for the investigation of topically applied substances into the hair follicles?," *Skin Pharmacol. Physiol.* **23**(1), 47–52 (2010).